Reorientation dynamics in thin glassy films

Reorientation dynamics in thin glassy films

E Cecchetto, D Moroni and B Jérôme

Van 't Hoff Institute for Molecular Sciences (HIMS), University of Amsterdam, Nieuwe
Achtergracht 166, 1018WV Amsterdam, The Netherlands

E-mail: cecchetto@science.uva.nl

Abstract
We present a study of orientational relaxation dynamics in thin films of a low-
molecular-weight glass former as a function of temperature and film thickness.
The relaxation is probed by means of second-harmonic generation after release
of a poling electric field. From the measured decays of the second-harmonic
signal and their fitting with a stretched exponential, we can determine the
distribution of relaxation times in the system. As temperature decreases from
above the glass transition, we observe that the width of the distribution first
increases under confinement, but that deeper in the glassy state, confinement
has no effect any longer on the dynamics.

1. Introduction

In the liquid phase of glass formers, the viscosity and any sort of relaxation time increase
enormously upon cooling. Relaxation times eventually become longer than the experimental
timescale, which is essentially the time during which the system is allowed to equilibrate after
a change of an external parameter or constraint. As a consequence, no changes are observable
any longer in the system and the structural configuration of the liquid appears to freeze below
the so-called glass transition temperature T_g. A deep understanding of the nature of the glass
transition is still lacking and reaching it is a challenging goal. Many theories have been
proposed [1–5] and revisited, but all fail to explain the whole collection of typical features
of the glass transition. Somehow each theory applies to a limited range of conditions, either
thermodynamic or kinetic.

One of the widely used theories of the glass transition is that of Adam and Gibbs [6],
which is based on the concept of cooperatively rearranging regions (CRRs). According to this
model, as the temperature of a liquid decreases toward the glass transition, the motion of the
molecules is no longer independent, but the dynamics becomes correlated over a certain number
of molecules. The spatial extent of this correlation is generally defined as the cooperative
length ξ. Parallel to the development of theories based on the idea of cooperative motion,
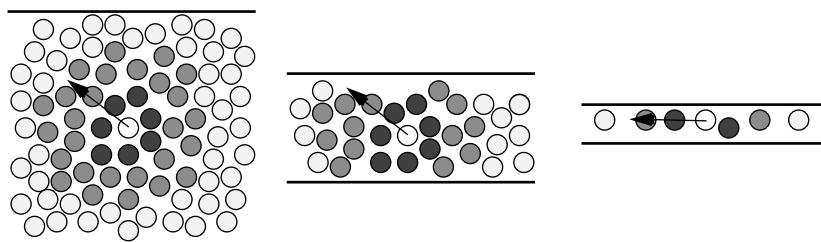
Figure 1. Schematic representation of the effect of confinement on cooperative motion: as the size of the system decreases, cooperatively rearranging regions (the radius of which is indicated by the arrow) get modified, and hence also the dynamics of the system.

other models focused on explaining the fact that the dominant α-relaxation is highly non-exponential. This non-exponentiality can be related to the superposition of relaxation processes with different relaxation times associated with different regions in the material, the so-called dynamic heterogeneities. The concept is indeed related to the CRRs, which can be considered as fast relaxing regions surrounded by slow or immobile molecules [7]. So the length scale of heterogeneities and the cooperative length should essentially be the same. Both simulation and experiments have been used to provide evidence for the existence of such a length scale and to evaluate it (see e.g. [7–12]). The values obtained at T_g or just above it are of the order of a few nanometres, both for low-molecular-weight and polymeric systems. Theories predict that this length should increase as temperature decreases.

The concept of cooperativity suggests that the dynamics of glass formers should be modified if the size of the system becomes comparable to the cooperative length ξ. In this size range, it is the size of the system that determines the size of cooperatively rearranging regions (figure 1) and therefore the dynamic behaviour of the system. So one expects modifications of the dynamics, namely of the distribution of relaxation times and the glass transition temperature, in glassy systems with sizes in the mesoscopic range. Taking into account only pure geometrical effects (without interactions with walls) and assuming the presence of cooperatively rearranging regions of size ξ, we can expect the following changes in the dynamic behaviour of glass formers when they are confined in thin films [13]. For thicknesses rather large with respect to ξ, confinement only affects molecules in the vicinity of the surfaces (figure 1). Surface molecules belong to cooperatively rearranging regions that are smaller than the ones present in the bulk. Therefore their relaxation should be faster than that of molecules in the middle of the system. As the size of the system decreases, the proportion of molecules affected by the surfaces increases. As a consequence, the distribution of relaxation times in the system should broaden toward the short timescales leading to a decrease of the mean relaxation time. When the film thickness becomes comparable with ξ, all molecules are affected by confinement and the size of the cooperatively rearranging regions is determined by the size of the system. Decreasing the size even more down to a molecular size will make the system homogeneous again, with all molecules having essentially the same environment. However, the relaxation time will be smaller than the value in the bulk, because the motion of the molecules becomes essentially individual again.

Research on the effect of confinement on glass dynamics has concentrated on two kinds of systems: low-molecular-weight glass formers in porous media and polymers in thin films. In low-molecular-weight glass formers, as measured by dielectric spectroscopy, the characteristic time corresponding to the α orientational relaxation is generally decreasing and the distribution of relaxation times broadens as the size of the system decreases [14–17]. From the effects of
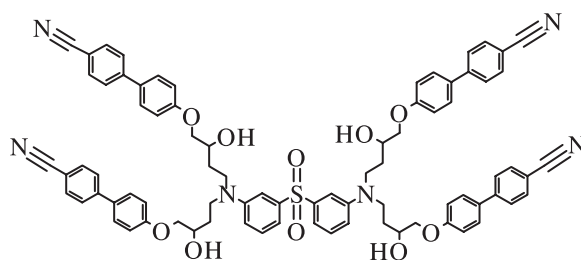
Figure 2. Chemical structure of the glass former.

size on the dynamics, it is possible to make an estimate of the cooperative length ξ. The value of ξ for salol in the vicinity of the calorimetric glass transition temperature was estimated to be $\geqslant 70$ Å [15]. Similar values of ξ at T_g were obtained for propylene glycol, with $\xi \leqslant 60$ Å, and for N-methyl-ϵ-caprolactam ($\xi \leqslant 120$ Å) [18]. Confinement in porous media, however, introduces curvature effects and is not well defined in size because of the polydispersity in pore sizes and the presence of pore junctions. These problems are avoided in thin films, which have so far only been used for polymeric systems. In free-standing films, the mean relaxation time was found to be significantly lower than in the bulk while the relaxation dynamics followed the same stretched exponential as in the bulk [19]. In contrast a significant broadening of the distribution of the relaxation times has been observed in films supported by a substrate [20, 21]. There has also been one study of the effect of confinement on the width of the distribution of the relaxation times as a function of temperature in a side-chain polymer [20]. It was found that, at all temperatures, the average relaxation time is essentially independent of the film thickness, while the width of the distribution of the relaxation times increases as thickness decreases. The widening of the distribution was however found to be the same over the whole temperature range considered ($T_g - 13\,°C < T < T_g + 25\,°C$). Studies on polymers then have not shown so far any clear trend. Because of their chain character, polymers exhibit bulk dynamic processes and a behaviour under confinement that is specific to these materials rather than glasses in general.

To overcome these problems, we have studied the dynamic behaviour of low-molecular-weight glass formers in thin films. To our knowledge there is no study reported in the literature on the dynamics of low-molecular-weight systems in as simple a confining geometry as thin films. We have chosen a hydrogen-bonded glass former, with a fairly simple chemical structure (see figure 2), for which we can expect relatively simple relaxation processes. Moreover, small molecules can be obtained with a higher chemical purity and without molecular weight or composition distribution. The small size of our compound has however the disadvantage that the characteristic lengths in the system should be smaller than in polymeric systems. As a consequence, confinement effects will appear at smaller film thicknesses.

In previous measurements performed with x-ray reflectivity [22], we have seen one effect of confinement on a glass former into a thin film: the glass transition significantly widens. This was interpreted as originating from an increase of the inhomogeneity of the dynamics in the system. To obtain direct evidence for the variation of the inhomogeneity under confinement and study in detail how confinement affects the dynamics of the system, we have examined the reorientation dynamics of our low-molecular-weight glass former in thin films, starting from an initial state imposed by an external field. The dynamics has been followed experimentally over a wide range of temperatures around T_g, an extended time window and for confining sizes down to a few molecular units, which is expected to be of the order of ξ. The temperatures are equally
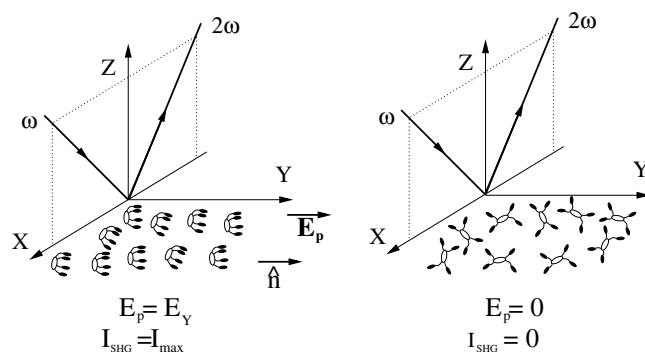
Figure 3. Schematic representation of the orientation order of the polar branches in the glass former with an applied poling field (left) and after removal of the field and complete relaxation (right). The poling field $\mathbf{E}_Y$ is perpendicular to the optical plane (XZ) defined by the incident and second-harmonic beams.

distributed between $T_{g,\mathrm{DSC}} - 46\,^\circ\mathrm{C}$ and $T_{g,\mathrm{DSC}} + 14\,^\circ\mathrm{C}$ ($T_{g,\mathrm{DSC}}$ indicates T_g as measured by differential scanning calorimetry), resulting in a few temperatures above and even more below the thermal glass transition temperature. We have used the optical second-harmonic generation technique to follow the reorientation process. Second-order non-linear optical effects, such as second-harmonic generation, are in principle forbidden in centrosymmetric media [23, 24]. It is therefore particularly suitable to follow the reorientation dynamics between an initial polar state and a final non-polar state. The principle of the experiment is the following: the films to be studied are first brought into the liquid phase and a strong DC poling field $\mathbf{E_p}$, parallel to the film plane, is then switched on. This field tends to align the dipoles carried by the side-groups along the direction of the field (figure 3). In this polar state, the sample generates a high second-harmonic (SH) signal. At a time $t = 0$, we switch the poling field off and follow the reorientation of the dipoles toward an isotropic in-plane distribution of dipole orientations through the decay of the second-harmonic signal in time. Other glassy systems have already been studied with this experimental method [20, 25–28], most of them being polymeric materials. In [25] for instance, the measurements probe the reorientation dynamics of a chromophore that is either dissolved in the hosting material or attached to the polymer main chain by a flexible spacer.

In the following, we start by describing our samples and experimental technique (section 2). We then present our results on the reorientation dynamics in the glassy films and how it is affected by changes in the size of the system (section 3), and finally discuss these results (section 4).

2. Experimental details

2.1. Samples

For the relaxation measurements we have used $4'$-(4-[3-(3-bis-[4-($4'$-cyano-biphenyl-4-yloxy)-3-hydroxy-butyl]-amino-benzenesulfonyl)-phenyl]-[4-($4'$-cyano-biphenyl-4-yloxy)-3-hydroxy-butyl]-amino-2-hydroxy-butoxy)-biphenyl-4-carbonitrile (see figure 2). The material ($T_{g,\mathrm{DSC}} = 106/110\,^\circ\mathrm{C}$ as measured by DSC at 20 K min^{-1}) [29, 30] belongs to the polyalcohols family. This family is characterized by the presence of hydroxy functional groups that are known to create H-bonded networks. In the plot of the relaxation time versus T_g/T, as

originally constructed by Angell [31, 32], alcohols [33] and polyalcohols [34] are found to occupy the intermediate region between strong and fragile glass formers.

Low-molecular-weight glass formers do not allow preparation of free-standing films, and we thus employed supported thin films obtained by spin coating from a cyclopentanone solution on fused quartz substrates. The thickness (100–1200 Å) and quality of these films were characterized by x-ray reflectivity [22, 35] and atomic force microscopy [35]. The film–substrate interaction was previously studied by following the expansion behaviour of the liquid phase of the glass former and was found to be negligible [22]. It had already been observed by means of x-ray reflectivity that films of the same compound with a thickness between 40 and 100 Å become unstable during the first heating and break up into droplets [36].

To enable application of an electric field parallel to the substrate, the quartz plates were first patterned with two planar electrodes separated by a gap d of 1 mm. The electrodes were obtained by first depositing a thin (10 nm) layer of chromium, which has a high affinity for silica, and then depositing a second thick (100 nm) gold layer. A high DC electric field was applied between the two electrodes. For poling the films, we used a constant voltage V of 1.9 kV. The electric field produced in the gap is perpendicular to the electrode edges and parallel to the substrate surface. The intensity profile of this field depends on the distance from the edges [37]. In the middle of the gap the electric field is minimum and equal to $E_p = \frac{2}{\pi} \frac{V}{d}$, which corresponds to 1.2×10^6 V m^{-1}. Around this minimum the field is constant within 1% in a region of width $d/5 = 200$ μm in our case. This width is sufficiently large for our measurements, which are all performed with a projected laser beam area of ~ 100 μm in diameter. We assume therefore that the electric field is uniform in the probed surface area. The degree of polar ordering induced by the poling field is proportional to the applied field. Therefore a higher field is expected to increase the ordering and the initial SH signal before the field is switched off. Nevertheless we have to limit the applied voltage to 1.9 kV because higher fields cause arching between the two electrodes, which destroys the samples. The high-voltage power supply limited the current during the transient regime just after switching the electric field on or off to 10 mA.

2.2. Measurements

The reorientation of the dipoles has been followed measuring the second-harmonic signal after switching off the poling field $\mathbf{E_p}$. We have measured the second-harmonic signal with an incoming light and SH signal both having s polarization (s = Y in figure 3, s-in–s-out) perpendicular to the incident plane (XZ in figure 3). On releasing of the field at time $t = 0$, the field-induced orientational order disappears in the course of time by the randomization of the orientations of the dipoles. This leads to a decrease of the SH signal to zero. So the reorientation dynamics of the system can be followed by measuring the SH signal I_{ss}. The square root of the I_{ss} is directly proportional to the degree of polar ordering in the system through the effective susceptibility χ_{ss} of the film [38].

With the above measurement method, the state from which the relaxation starts is determined by the applied poling field. For the range of poling fields we have used, $\chi_{ss}(0)$ is proportional to the field strength [20, 39, 40]. In principle, the measured relaxation times can be expected to depend on the degree of order of the starting state of the relaxation, and thus on $\mathbf{E_p}$ [41]. We have not studied this dependence and have used only one value of $\mathbf{E_p}$.

For the second-harmonic generation measurements we have used a frequency-doubled Q-switched mode-locked Nd-YAG laser (Antares 76, Coherent) as light source with an output wavelength at 532 nm, using an s-in–s-out polarization configuration (for more details see [35]). The repetition rate of the Q-switched pulses was tuned between 50 and 200 Hz depending on

the timescale at which the relaxation process was explored. A special set-up was developed to trigger and delay the switching of the external poling electric field with respect to the optical Q-switched pulses in order to reach timescales for the relaxation process down to 1 μs [35, 42]. The Q-switched pulse energy was at most 1 mJ, which is not high enough to induce molecular reorientation. We have also checked that the laser does not influence the dynamics of the system by heating it.

2.3. Thermal history

To eliminate the solvent from the deposited films, samples were first annealed at 45 °C for 5 h. They were then heated above the glass transition to 120 °C where they were kept for at least 15 min. To facilitate solvent removal and provide a clean atmosphere, the sample chamber was fluxed continuously with dry nitrogen. After switching on the external field the temperature was brought to the desired value and then kept constant during the experiment. All temperature ramps were conducted at 0.25 K min^{-1}. This cooling rate range was found to minimize ageing effects on film thickness behaviour [22].

At time $t = 0$, when the desired temperature was reached, data points were collected according to two different protocols for fast and slow relaxations. For times between 5 μs and 3 s repeated on/off cycling of the external field allows multiple measurements of the reorientation dynamics. During the overall collection time, we observed no trend in the SH signal, and thus no evidence of ageing. For longer timescales, up to 72 h, the electric field was switched off permanently at time $t = 0$ and a single collection measurement was performed. Enhanced statistics was acquired by repeating the whole sampling preparation. This protocol might be affected by ageing, especially at temperatures well below T_g, where the dynamics is slower. All measurements were averaged over a few thousand repeated collections to increase the signal to noise ratio using a home-developed collection protocol [35, 42].

As a result of the combination of the two protocols, the relaxation functions are determined over a range of 11 orders of magnitudes in time from 1 μs upward. The ability to characterize reorientation dynamics over a wide range of timescales is crucial for determining accurately the fitting parameters of the relaxation function.

2.4. Data analysis

The measured values of the effective susceptibility χ_{ss} of the film are normalized to the value before the switching off of the poling field ($\chi_{ss}(0)$) and fitted using the phenomenological stretched exponential Kohlrausch–Williams–Watts (KWW) response function [2]:

$$\chi_{NO}(t) = \frac{\chi_{ss}(t)}{\chi_{ss}(0)} = \exp(-(t/\tau_W)^{\beta_W}) \tag{1}$$

where τ_W is a characteristic decay time and $0 < \beta_W \leqslant 1$ is the stretch exponent. This non-exponential relaxation function is generally associated with a distribution of pure exponential relaxations spread through the system [43]. The system is then considered as a set of relaxators i, which can be visualized as nanoscopic regions within the glass former, each one with a defined time constant τ_i. The observed relaxation results from their superposition:

$$\chi_{NO}(t) = \sum_i G(\tau_i) \exp(-t/\tau_i) \tag{2}$$

where the weight of relaxator i is given by $G(\tau_i)$, more often written as a continuous distribution function $G(\tau)$ where τ is a variable for the relaxation times and is not to be confused with the KWW parameter τ_W.

In the general case when the form of $\chi_{NO}(t)$ is arbitrary, the two functions $\chi_{NO}(t)$ and $G(\tau)$ are uniquely derived from one another through an operation involving a Laplace transform [44]. In the case when $\chi_{NO}(t)$ follows the KWW law, $G(\tau)$ is directly determined by the two parameters τ_W and β_W. $G(\tau)$ can then be written in the form of a definite integral or a series, but there is no analytical solution except for the cases $\beta_W = 1/2$ and 1.

The distribution function $G(\tau)$ is numerically computed using a recursive computer algorithm developed by Emri and Tschoegl [45], and often applied to interpret SHG decays [20, 46, 47]. The maximum of $G(\tau)$ corresponds approximately to τ_W and its breadth is related to $0 < \beta_W \leqslant 1$. The smaller β_W the wider the distribution, the special case $\beta_W = 1$ corresponding to a single-exponential relaxation and a delta function $G(\tau)$.

3. Results

We have examined the dependence of the reorientation dynamics as a function of two parameters: temperature and film thickness. In the following, we first present the results concerning the temperature dependence of the dynamics in a thick film (as-spun thickness $h_0 = 116$ nm). From the thermal expansivity measurements we have presented in [22], we expect a bulk-like behaviour for the molecular dynamics of such a thick film. We can therefore compare our dynamic measurements with the expected behaviour around the glass transition temperature of a bulk glassy system. Next we examine how the dynamics at different temperatures is affected as the film thickness decreases. From the broadening of the glass transition we have reported in [22], which is a sign of an increased inhomogeneity of the film, we expect a broadening of the distribution of the relaxation times as the film thickness decreases.

3.1. Temperature dependence of relaxation dynamics in thick films

In figure 4 we plot the time dependence of the effective non-linear susceptibility χ_{ss} normalized to its value before the poling field is switched off at time $t = 0$, for a 116 nm thick film. We show for clarity the results only for the temperatures just below (100 °C) the *nominal* bulk glass transition temperature determined by DSC ($T_g = 106$ °C) and deep into the glass phase (60 °C). From the observed decays it is clear that any contribution to χ_{ss} from electric-field-induced second-harmonic (EFISH) generation [40, 42, 48] can be neglected. Indeed, for all temperatures, the SH signal does not decrease for several decades in time. A possible contribution of EFISH generation would result in an immediate jump of the signal to a lower value, as fast as the poling field $\mathbf{E_p}$ drops to zero ($\sim$100 ns). We conclude, then, that the observed decays are associated solely with reorientation dynamics of the non-linearly polarizable units of the molecules.

Data are fitted with the stretched exponential KWW law given by equation (1). The characteristic time τ_W and the stretch exponent β_W obtained at the different temperatures are given in table 1. The values of β_W exhibit little temperature dependence. As they are significantly different from 1, it is obvious that the relaxation process is highly non-exponential.

Another way to characterize the dynamic behaviour of the system is to calculate an average reorientation time $\langle \tau \rangle$ as is generally done for polymer systems from dynamic optical or dielectric measurements [10, 26, 49–51]:

$$\langle \tau \rangle = \int_0^\infty \exp\left[-\left(\frac{t}{\tau_W}\right)^{\beta_W}\right] dt = \frac{\tau_W \Gamma(1/\beta_W)}{\beta_W} \tag{3}$$

where Γ is the gamma function. For $\beta_W = 1$ (single exponential), $\langle \tau \rangle$ is equal to τ_W. This parameter is however not only dependent on the characteristic time τ_W but also on the shape
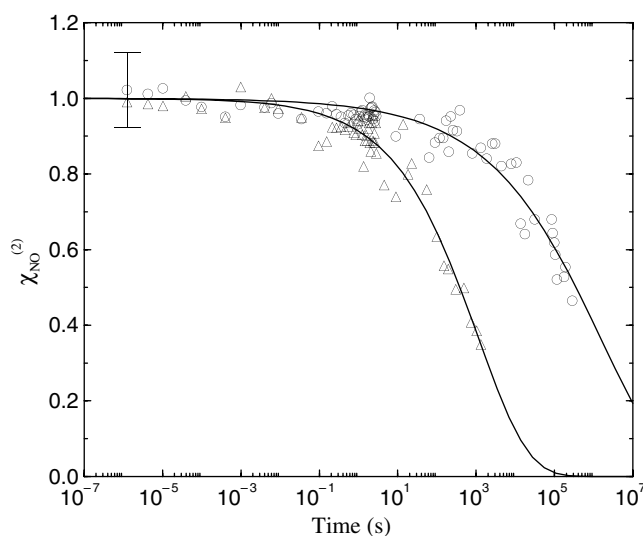
Figure 4. Normalized second-order susceptibility versus time for a 116 nm thick film (as-spun thickness) at (●) 60 °C ($T_g - 46$ °C) and (△) 100 °C ($T_g - 6$ °C). Solid lines represent the best least-squares fit using equation (1). Displayed error bars at 60 °C are similar for all temperatures and delay times.

Table 1. Values of the characteristic time τ_W and stretch exponent β_W obtained by fitting the experimental relaxation with equation (1), and average relaxation $\langle\tau\rangle$ time calculated with equation (3), for the different temperatures and thicknesses considered.

$h(0)$ (nm)	T (°C)	τ_W (s)	β	$\langle\tau\rangle$ (s)
116	60	1.46×10^6	0.26	29×10^6
	80	36×10^3	0.32	250×10^3
	90	16×10^3	0.28	220×10^3
	100	1.1×10^3	0.34	6.2×10^3
	120	160	0.31	1.24×10^3
70	100	2.5×10^3	0.31	20.5×10^3
41	100	6.4×10^3	0.30	62×10^3
25	100	1.5×10^3	0.27	25×10^3
17	60	1.5×10^6	0.24	43×10^6
	120	160	0.32	1.1×10^3
	130	39	0.56	65
10	60	6×10^6	0.26	110×10^6
	90	5.9×10^3	0.22	320×10^3
	100	2.8×10^3	0.21	190×10^3
	110	610	0.28	7.8×10^3

of the distribution of the relaxation times. The results for the 116 nm thick film are also given in table 1. For all temperatures, $\langle\tau\rangle$ is rather large. Even for the highest temperature ($T = 120$ °C $= T_g + 14$ °C) the average relaxation time lies above the value generally associated with the macroscopic glass transition $\langle\tau\rangle_{T_g} = 100$ s [2].

From the KWW fitting parameters τ_W and β_W we have computed the distribution functions of relaxation times $G(\tau)$ as explained in section 2.4 (figure 5). The measured relaxation decays

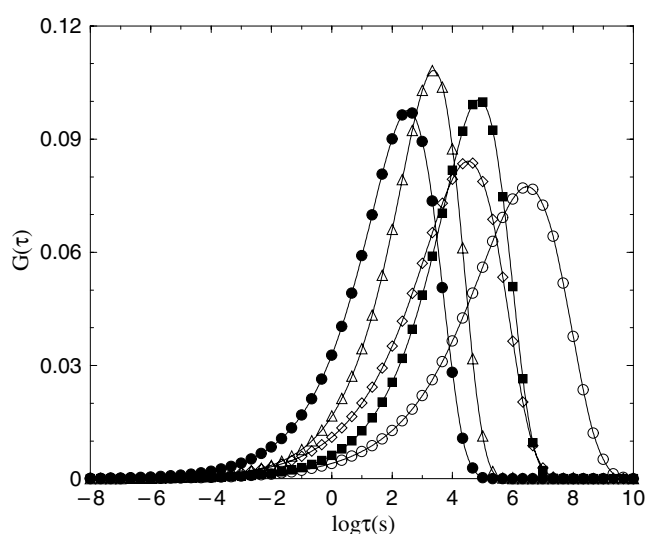**Figure 5.** Distribution of relaxation times calculated for a 116 nm thick film from the parameters given in table 1: 60 °C (O), 80 °C (■), 90 °C (◇), 100 °C (△) and 120 °C (●). The solid lines are only a guide to the eye.

at low temperatures do not decay to 0 at the largest experimental time (figure 4). Calculating the distribution of relaxation times using the high characteristic time τ_W evaluated with the KWW fitting law (equation (2)) introduces weights $G(\tau_i)$ for times τ_i longer than the measured ones. Thus the contributions to the distribution function at times $\log(\tau) > 6$ have to be taken as purely a result of the computation but not directly related to the experimental measurements. The calculations of $G(\tau)$ confirm the trend indicated by table 1 for the average relaxation time and the width of the distribution. For the film thickness considered, the width of the distribution does not show a particular trend at temperatures larger than 80 °C. Only at the lowest temperature measured (60 °C) is a slight widening of the distribution visible. When the temperature increases, the peaks of the distribution move from long to short times by almost four orders of magnitude in time in the explored temperature window. Note that the characteristic time τ_W corresponds approximately to the maximum of the distribution, while the average calculated with equation (3) is equal to the average calculated from the distribution $G(\tau)$. This confirms the consistency of our data analysis.

The wide distributions of relaxation times shown in figure 5 confirm the fact that to make an accurate evaluation of the distribution $G(\tau)$, experimental relaxation decays covering many orders of magnitude in time are needed. Indeed, the relaxation time distributions cover 14 orders of magnitude in time (10^{-4}–10^{10} s) for the range of temperatures studied.

3.2. Thickness dependence of the relaxation dynamics

To investigate the effect of confinement we carried out the same relaxation experiment as is presented in section 3.1 for films with a lower thickness. In figure 6 we show the signal decay measured at 120 and 60 °C for a 17 nm thick film (as-spun thickness).

The decay measured at 120 °C presents an interesting feature: the SH signal exhibits a first decay in the short time domain. The use of the KWW equation to fit the data appears to be only a first approximation. The data are not properly described in the ms time window and
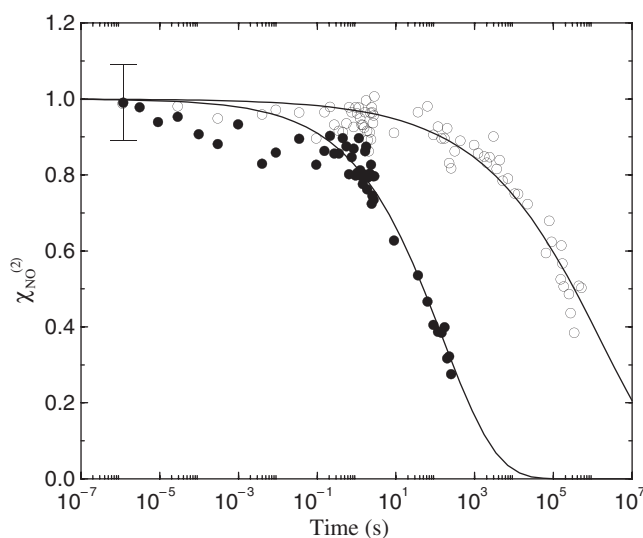
Figure 6. $\chi_{NO}^{(2)}$ versus time for a 17 nm thick film (as-spun) at (○) 60 °C ($T_g - 46$ °C) and (●) 120 °C ($T_g + 14$ °C). Solid lines represent the best least-squares fit using equation (1). Displayed error bars at 120 °C are similar for all temperatures and delay times.

a general double-stretched-exponential law would be more suitable. It seems that, under our experimental conditions, it is possible to discriminate different relaxation processes. Measuring relaxation dynamics around and below the bulk glass transition means in principle probing the α-relaxation process. Nevertheless, at high temperatures, the α-process does not necessary screen all other faster processes. These modes observed at high temperature can have different origins. One possible interpretation is to attribute this mode to the fast β-process, related to a local mobility.

However, given the small contribution of possible fast processes (observed only at high T), we fitted in first approximation all decays with a single stretched exponential function using equation (1). Fitting with a double stretched exponential the data at high T hardly changes the parameters for the α-process. The resulting fitting parameters τ_W and β_W together with the calculated average relaxation time $\langle\tau\rangle$ are reported in table 1. The corresponding distribution of relaxation times $G(\tau)$ is plotted in figure 7.

An interesting feature is the increase of the exponential character (increase of β_W) for the highest temperature measured, which results in a sharper distribution of relaxation times for $T = 130$ °C in figure 7. Note that for this temperature the distribution function moves toward shorter times and $\langle\tau\rangle < 100$ s.

To increase the effect of confinement, we repeated the above experiments with an even thinner film (10 nm). The only difference with the thicker films was that the annealing temperature was 110 °C instead of 120 °C, due to the instability of the film at higher temperatures. The fitting parameters of the SH decays for four different temperatures are presented in table 1. The calculated distribution of relaxation times are shown in figure 8. As temperature increases, the peak in the distribution shifts uniformly towards shorter times to 100 °C. Notice in figure 10 that β_W first decreases and then increases slightly as the temperature decreases, having the minimum at around 100 °C ($T_g - 6$ °C).

At this temperature we have also collected the relaxation decay for 25, 41 and 70 nm thick films. The distribution of relaxation times $G(\tau)$ of all the measured films at 100 °C is plotted in figure 9.
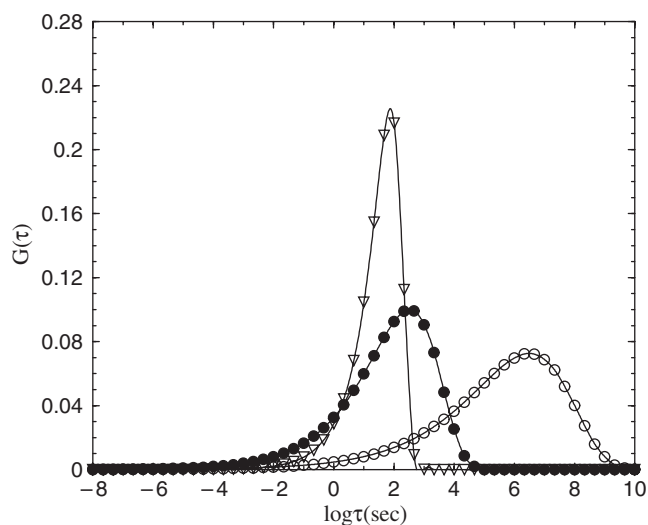
Figure 7. Distribution of relaxation times for a 17 nm thick film from the parameters in table 1: 60 °C (○), 120 °C (●) and 130 °C (▽). The solid lines are a guide to the eye.
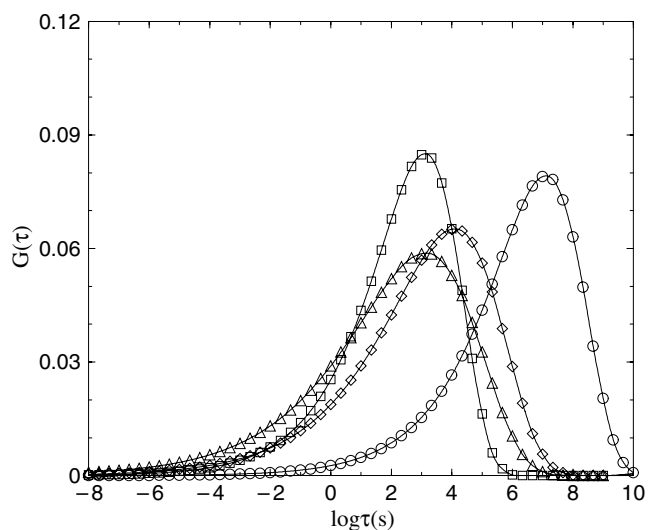

Figure 8. Distribution of relaxation times for a 10 nm thick film from the parameters in table 1: 60 °C (○), 90 °C (◇), 100 °C (△) and 110 °C (□). The solid lines are a guide to the eye.

4. Discussion and conclusion

We summarize our results on the dynamics of thin films by plotting the temperature dependence of the stretch exponent β_W (figures 10 and 11), the characteristic time τ_W (figure 12) and the average relaxation time $\langle \tau \rangle$ (figure 13).

The first important issue arising from these measurements is whether the measured reorientation dynamics of the non-linearly polarizable groups is coupled with any glassy dynamics of the molecules as a whole. The reorientation of the non-linearly polarizable
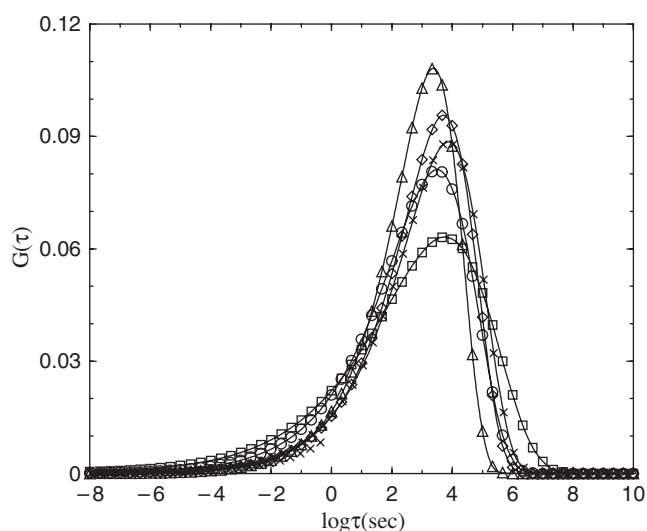
Figure 9. Distribution of relaxation times at $100\,^{\circ}\mathrm{C}$ ($T_\mathrm{g} - 6\,^{\circ}\mathrm{C}$) for a 10 nm ($\square$), 25 nm ($\bigcirc$), 41 nm ($\times$), 70 nm ($\Diamond$) and 116 nm ($\triangle$) thick films. The solid lines are a guide to the eye.
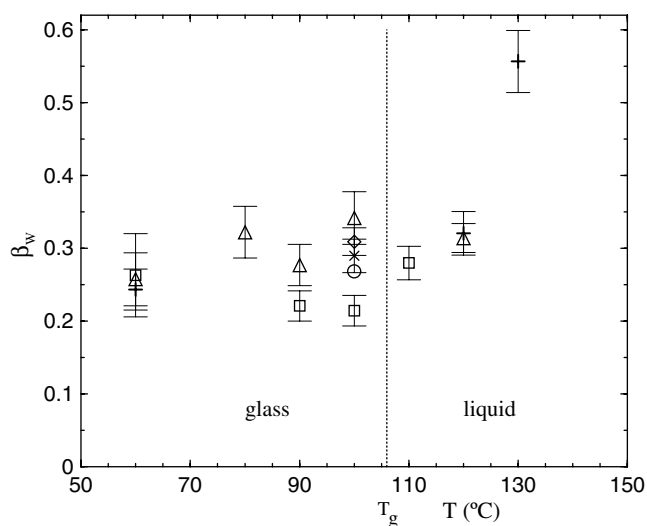
Figure 10. Stretch exponent β_W versus temperature for 10 nm ($\square$), 17 nm (+), 25 nm ($\bigcirc$), 41 nm ($\times$), 70 nm ($\Diamond$) and 116 nm ($\triangle$) thick films.

groups is probably strongly coupled to that of the rest of the molecules, since the flexible spacer between the central rigid group and the polarizable side-groups contains only three atoms (see figure 2). The fact that the reorientation dynamics of side-groups is coupled to the α-relaxation process has also been demonstrated in a polymeric system with a flexible spacer of four atoms [46]. The same coupling has also been demonstrated for chromophores dissolved in a polymer without any covalent bonding with the polymer chains [26]. However this could be due to strong steric interactions between the chromophores and the chains, which are less likely to take place in our low-molecular-weight glass former. The technique used
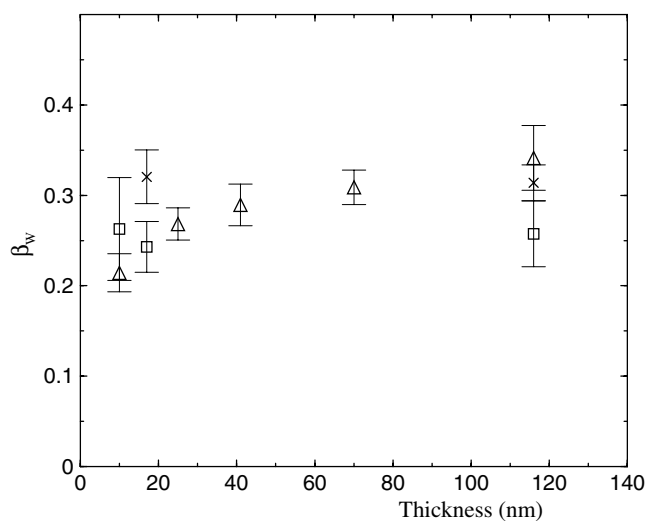
Figure 11. Stretch exponent β_W versus film thickness for 60°C ($\square$), 100 °C ($\triangle$) and 120 °C ($\times$).
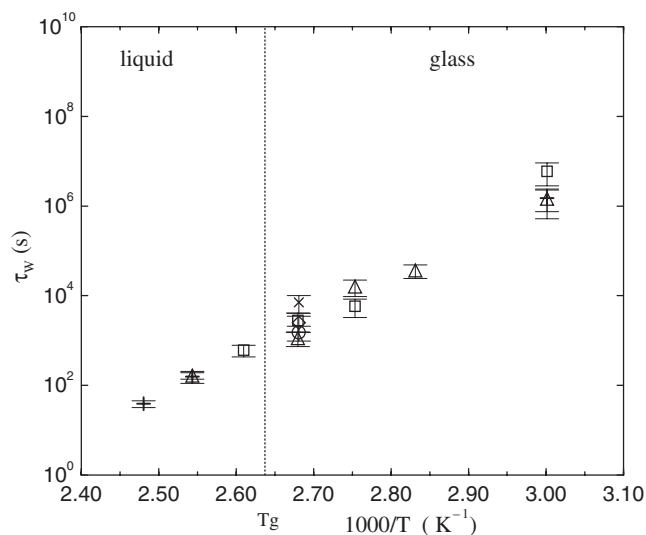

Figure 12. Characteristic time τ_W versus inverse temperature for 10 nm ($\square$), 17 nm (+), 25 nm (O), 41 nm ($\times$), 70 nm ($\Diamond$) and 116 nm ($\triangle$) thick films.

to study α-processes is usually extended also below T_g where it is generally believed that no α-relaxation takes place and there is no dynamic glass transition. The dependence of τ_W $(T < T_g)$ as a function of the inverse temperature shows an apparent Arrhenius behaviour, exponentially increasing with $1/T$. Our measurements (see figure 12) display this behaviour, and the activation energies for the thinnest and thickest film are similar within the error and equal to 45 kcal mol^{-1} as found for other glass formers [46]. Further evidence for the glassy character of our system can be found in the values of β_W for the thickest film exhibiting a bulk-like behaviour. The values are rather scattered but remain in the interval 0.25–0.35. If we take for the value at T_g the average of the measured values, we obtain $\beta_W(T_g) \sim 0.30$, which
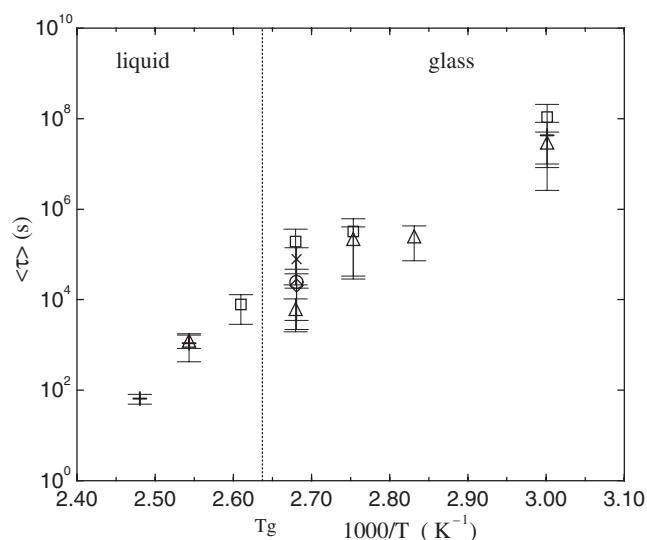
Figure 13. Average relaxation time $\langle\tau\rangle$ versus inverse temperature for 10 nm (□), 17 nm (+), 25 nm (○), 41 nm (×), 70 nm (◊) and 116 nm (△) thick films.

is close to the value for the bulk poly(propylene glycol) [31]. This can be expected from the fact that our compound carries four hydroxy groups per molecule and should belong to the most fragile hydrogen-bonded glass formers group. We thus conclude that the reorientation dynamics that we observe corresponds to the one expected for a glass former.

We also observe however deviations of the dynamics behaviour from the expectations on two points. One is that even at temperatures above the bulk glass transition temperature T_g (as measured by DSC), the average relaxation time $\langle\tau\rangle$ is longer than the one corresponding to the standard definition of T_g: $\langle\tau\rangle_{T_g} = 100$ s. In [22] we saw that there is no evident variation of T_g under confinement. So the high values of $\langle\tau\rangle$ cannot be explained by an increase of T_g. The origin of the long relaxation times might be related to the fact that the non-polarizable side-groups are polar mesogenic units. Ordinary non-glassy liquid crystals based on the same cyanobiphenyl units exhibit also a very slow reorientation dynamics in ultrathin films (thickness below 10 nm) [48, 52, 53]. The reason for this slow dynamics is not clear. One possible explanation could be the electrostatic correlation between the dipoles carried by the cyanobiphenyl groups [40], although no direct evidence for such a correlated dynamics has been found yet.

The second unexpected feature in the observed dynamics (in particular in thick films) is the fact that the time dependence of the observed relaxations remains strongly stretched at temperatures above the bulk glass transition temperature. We could expect an increase of the stretch exponent β_W indicating a narrowing of the distribution as temperature increases. The fact that we do not observe this narrowing might simply be due to the limited range of temperature that we can explore above T_g. When we did manage to perform experiments at slightly high temperatures (130 °C with the 17 nm thick film), we did indeed observe an increase of β_W. Similar results were found on polymer systems [26, 47, 54], where β_W does not vary significantly in the glassy phase, while for temperature above T_g, β_W was increasing with temperature.

Our experimental results allow a discussion on the main purpose of our study, namely the effect of confinement on the dynamics of glass formers. From the characteristic time τ_W

plot (figure 12) we can notice that at high and low temperature τ_W hardly depends on the film thickness. At intermediate temperatures around T_g, data are scattered without a specific variation with film thickness. Nevertheless the dispersion is limited, allowing us to state that τ_W is essentially independent of film thickness. In the same temperature interval, $\langle \tau \rangle$ (figure 13) shows an even wider scattering. This scattering comes from variations in the actual shape of the distribution of relaxation times $G(\tau)$, which can have a strong influence on $\langle \tau \rangle$ while the location of the maximum of $G(\tau)$ hardly moves. This can be seen in the plot of the distribution of relaxation times for different film thickness at $T = 100\,^\circ C$ (figures 9 and 11). Maxima are hardly shifted with respect to one another (less than one order of magnitude), but the asymmetric widening of $G(\tau)$ for the thin films leads to differences in $\langle \tau \rangle$ of two orders of magnitude. So confinement does not have much effect on the position of the peak of the distribution of relaxation times, but does have a significant effect on the width of this distribution, which is directly related to the stretch exponent β_W. The summary of the results in figures 10–13 shows that we can distinguish three temperature regions exhibiting different behaviours:

- *High temperatures* ($T \gtrsim 120\,^\circ C$). Although the number of measurements we could perform in this range is small, it is clear that thickness has little influence on the dynamics (see figures 11 and 12). This can be understood from the fact that at $120\,^\circ C$, in the liquid phase, the dynamics can only be little affected by size effects. Eventually the dynamics will be modified at small thickness (below 10 nm) by the presence of the free surface and film–substrate interface. The effect is quite likely not large enough to be observed with our experiments.

- *Intermediate temperatures* ($70\,^\circ C \lesssim T \lesssim 120\,^\circ C$). In this temperature range, there is an influence of the film thickness on the dynamics. The stretch exponent β_W of the thinnest film (10 nm) significantly decreases as temperature decreases and reaches a minimum at around $100\,^\circ C$ and then slightly increases again (figure 10). The decrease of β_W indicates a widening of the distribution of the relaxation times. Since this widening is not observed in the thickest film (116 nm thick) we can conclude that it is due to an increase of the inhomogeneity of the films under confinement. This is in agreement with our observation of a broadening of the glass transition as the film thickness decreases. To study the temperature dependence we plot in figure 11 β_W as a function of film thickness for different temperatures. The β_W values at $100\,^\circ C$ depend on film thickness while they are not a strong function of film thickness in the liquid ($120\,^\circ C$) and glassy state ($60\,^\circ C$). Note also that the temperature range in which β_W is decreased in the thinnest films, with respect to the value for thick films, corresponds to the temperature range in which the glass transition takes place in the thinnest films studied with x-ray reflectivity [22]. This is indeed the temperature range in which one expects the inhomogeneity to be the largest, with part of the film in the liquid state and the rest in the glassy state. Since the average relaxation time varies very rapidly in the vicinity of the glass transition, the difference between the dynamics in the different parts of the system is then the largest.

- *Low temperatures* ($T \lesssim 60\,^\circ C$). The difference in dynamics between films at different thicknesses diminishes as temperature decreases below $100\,^\circ C$ and becomes unmeasurable at approximately $60\,^\circ C$. Although we have not performed measurements at lower temperatures because the relaxation of the system becomes extremely long, we can expect this independence of temperature to also occur below $60\,^\circ C$.

  Following the argument in the discussion of the intermediate temperatures, we can say that $60\,^\circ C$ is the temperature at which the glass transition is completed in the whole film (for the thinnest films we have measured). The inhomogeneity of the dynamics induced

by confinement becomes then equal to or smaller than the intrinsic inhomogeneity of the dynamics in the bulk and thick films.

Our finding that β_W becomes independent of film thickness at low temperatures is in contrast with the results of Hall *et al* [20] on polymer films. They found little influence of temperature on the difference in value of β_W for thin and thick films. This might however be due to the fact that they only performed measurements for temperatures above $T_g - 10\,°C$, while we measured down to $T_g - 46\,°C$.

We should also mention that below T_g ageing effects might take place. Studies on polymers [46] using the same experimental technique have shown that ageing the system shifts the distribution of relaxation times, but does not influence the breadth of the distribution. We have not investigated in detail ageing effects at low temperatures in our low-molecular-weight glass former, but we think that they would not influence substantially our considerations on the behaviour of the β_W parameter.

In the above discussion, we have not considered the role of the cooperative length ξ and its temperature dependence. From the model presented in [55], we know that the existence of ξ introduces an inhomogeneity of the system for film thicknesses close to ξ. The original theory of Adam and Gibbs of cooperative motion [6] predicts a divergence of ξ at a temperature below T_g. This implies that ξ should increase as temperature decreases. This means that as temperature decreases, the effect of confinement on the heterogeneity of the dynamics should start appearing at larger thicknesses and, for a given thickness, the inhomogeneity should increase as temperature decreases. This is however not what we have observed. One explanation for this is that ξ does not increase as temperature decreases, or at least not much. This has actually been observed in colloidal suspensions using confocal microscopy [12, 56]. In such a system, the glass transition is obtained by increasing of the density of particles. The size of fast relaxing clusters (which can be compared to cooperatively rearranging regions) was found to remain constant when the density increased beyond the glass transition. Unfortunately, no data are available on the temperature dependence of ξ below T_g in molecular systems.

In the simple model we presented in [13], making the cooperative length ξ independent of temperature also makes the relaxation time in the bulk and the degree of inhomogeneity in the film independent of temperature. We could introduce a variation of relaxation time in the bulk with temperature in a phenomenological way by imposing the appropriate temperature dependence of the energy barrier per molecule that needs to be overcome for allowing a relaxation process [13]. There is however no obvious way of obtaining a dependence of the distribution of relaxation times in the films as a function of temperature in agreement with our experimental results. So the simple model based on the idea that motion is cooperative over a certain length scale is not able to explain all the dynamic features of thin glassy films, although it explains some of them qualitatively.

In conclusion, we have investigated how the distribution of relaxation times in a low-molecular-weight glass former is affected by confining the sample in a thin film. Our main finding is that the effect of confinement on the dynamics of the system is the largest around the glass transition temperature in the bulk and that this effect vanishes as temperature is further lowered deep in the glass phase.

Acknowledgment

References

[1] Götze W 1991 *Liquids, Freezing and Glass Transition* (*Les Houches Lectures 1989*) ed J P Hansen, D Levesque and J Zinn-Justin (Amsterdam: North-Holland)
[2] Jäckle J 1986 *Rep. Prog. Phys.* **49** 171
[3] Ediger M D, Angell C A and Nagel S R 1996 *J. Phys. Chem.* **100** 13200
[4] Sappelt D and Jäckle J 1993 *J. Phys. A: Math. Gen.* **26** 7325
[5] Long D and Lequeux F 2001 *Eur. Phys. J.* E **4** 371
[6] Adam G and Gibbs J H 1965 *J. Chem. Phys.* **43** 139
[7] Sillescu H 1999 *J. Non-Cryst. Solids* **243** 81
[8] Binder K 2000 *J. Non-Cryst. Solids* **274** 332
[9] Glotzer S C *et al* 1998 *Phys. Rev.* E **57** 7350
[10] Schmidt-Rohr K and Spiess H W 1991 *Phys. Rev. Lett.* **66** 3020
[11] Russell E V and Israeloff N E 2000 *Nature* **408** 695
[12] van Blaaderen A and Wiltzius P 1995 *Science* **270** 1177
[13] Jérôme B 1999 *J. Phys.: Condens. Matter* **11** A189
[14] Schüller J, Richert R and Fischer E W 1995 *Phys. Rev.* B **52** 15232
[15] Arndt M *et al* 1997 *Phys. Rev. Lett.* **79** 2077
[16] Daoukaki D *et al* 1998 *Phys. Rev.* B **58** 5336
[17] Streck C, Mel'nichenko Y B and Richert R 1996 *Phys. Rev.* B **53** 5341
[18] Pissis P *et al* 1998 *J. Non-Cryst. Solids* **235** 449
[19] Forrest J A *et al* 1998 *Phys. Rev.* E **58** R1226
[20] Hall D B, Hooker J C and Torkelson J M 1997 *Macromolecules* **30** 667
[21] Fukao K *et al* 2001 *Phys. Rev.* E **64** 051807
[22] Cecchetto E, de Souza N R and Jérôme B 2000 *J. Physique* IV **10** Pr7
[23] Shen Y R 1989 *Nature* **337** 519
[24] Heinz T F 1991 *Nonlinear Surface Electromagnetic Phenomena* ed H E Ponath and G Stegeman (Amsterdam: Elsevier Science Publishers B.V.) chapter 5, pp 353–416
[25] Hall D B, Hamilton K E, Miller R D and Torkelson J M 1999 *Macromolecules* **32** 8052
[26] Dhinojwala A, Wong G K and Torkelson J M 1993 *Macromolecules* **26** 5943
[27] Pauley M A, Guan H and Wang C 1996 *J. Chem. Phys.* **104** 6834
[28] Fiestone M A, Ratner M A and Marks T J 1995 *Macromolecules* **28** 6296
[29] The glass formers have been provided by Akzo-nobel (Arnhem, The Netherlands); de Wit P P, Erdhuizz E W P and Picken S J *Patent* WO 96/0347
[30] A second batch was synthesized by Jager W and Kouwer P in the Polymer Materials and Engineering group at the University of Delft
[31] Böhmer R, Ngai K L, Angell C A and Plazek D 1993 *J. Chem. Phys.* **99** 4201
[32] Angell C A 1985 *J. Non-Cryst. Solids* **73** 1
[33] Cole R H and Davidson D W 1952 *J. Chem. Phys.* **20** 1389
[34] Angell C A and Smith 1982 *J. Phys. Chem.* **86** 3845
[35] Cecchetto E 2003 Molecular dynamics in thin glassy films *PhD Thesis* University of Amsterdam
[36] Demirel A L and Jérôme B 1999 *Europhys. Lett.* **45** 58
[37] Stähelin M *et al* 1993 *J. Appl. Phys.* **73** 8471
[38] Feller M B, Chen W and Shen Y R 1991 *Phys. Rev.* A **43** 6778
[39] Wang C H, Gu S H and Guan H W 1993 *J. Chem. Phys.* **99** 5597
[40] Schuddeboom P C, Meister R, Cecchetto E and Jérôme B 2003 *Eur. Phys. J.* E **11** 37
[41] Guan H W, Wang C H and Gu S H 1994 *J. Chem. Phys.* **100** 8454
[42] Cecchetto E, Collignon P and Jérôme B 2005 submitted
[43] Donth E 2001 *The Glass Transition, Relaxation Dynamics on Liquids and Disordered Materials* (Berlin: Springer)
[44] Lindsey C and Patterson G 1980 *J. Chem. Phys.* **73** 3348
[45] Emri I and Tschoegl N W 1993 *Rheol. Acta* **32** 312
[46] Dhinojwala A, Hooker J C and Torkelson J M 1995 *ACS Symp. Ser.* **61** 318
[47] Hall D B, Dhinojwala A and Torkelson J M 1997 *Phys. Rev. Lett.* **79** 103
[48] Schuddeboom P C, Meister R and Jérôme B 2001 *Mol. Cryst. Liq. Cryst.* **358** 139
[49] Reinsberg S A *et al* 2001 *J. Chem. Phys.* **114** 7299
[50] Russina M *et al* 2000 *Phys. Rev. Lett.* **84** 3630
[51] Chen S H, Mastrangelo J C and Shi H 1995 *Macromolecules* **28** 7775

[52] Schuddeboom P C 1998 Orientation of liquid crystal molecules at surfaces *PhD Thesis*
    University of Amsterdam
[53] Jérôme B, Schuddeboom P C and Meister R 2002 *Europhys. Lett.* **57** 389
[54] Dhinojwala A, Wong G K and Torkelson J M 1992 *Macromolecules* **25** 57395
[55] Dhinojwala A, Wong G K and Torkelson J M 1994 *J. Chem. Phys.* **100** 6046
[56] Week E R *et al* 2000 *Science* **287** 627